ACS POLYMERS Au
AN OPEN ACCESS JOURNAL OF THE AMERICAN CHEMICAL SOCIETY

pubs.acs.org/polymerau
Article

Continuous Polymer Synthesis and Manufacturing of Polyurethane Elastomers Enabled by Automation

Johann L. Rapp, Meredith A. Borden, Vittal Bhat, Alexis Sarabia, and Frank A. Leibfarth*

Cite This: ACS Polym. Au 2024, 4, 120−127
Read Online

ACCESS | Metrics & More | Article Recommendations | Supporting Information

ABSTRACT: Connecting polymer synthesis and processing is an important challenge for streamlining the manufacturing of polymeric materials. In this work, the automated synthesis of acrylate-capped polyurethane oligomers is integrated with vat photopolymerization 3D printing. This strategy enabled the rapid manufacturing of a library of polyurethane-based elastomeric materials with differentiated thermal and mechanical properties. The automated semicontinuous batch synthesis approach proved enabling for resins with otherwise short shelf lives because of the intimate connection between synthesis, formulation, and processing. Structure−property studies demonstrated the ability to tune properties through systematic alteration of cross-link density and chemical composition.

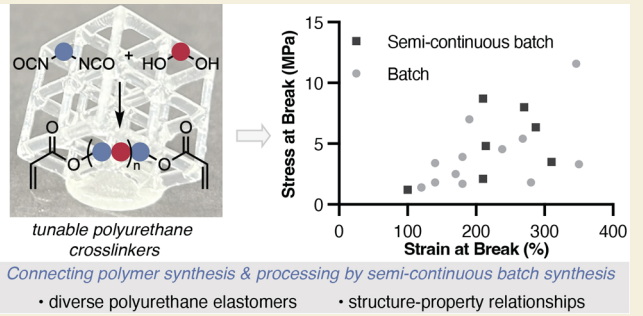

KEYWORDS: *additive manufacturing, polyurethanes, polymer networks, semiautomated batch synthesis, elastomers*

INTRODUCTION

Current approaches for plastics manufacturing decouple the synthesis of polymers and their subsequent processing into finished polymeric parts.[1] This workflow has largely been driven by economies of scale, where large quantities of polymer are synthesized at one location and shipped to many different processers. This centralized model, however, inherently limits the ability to tailor the synthesis to account for processing considerations or vice versa. Integrating polymer synthesis and processing into a continuous workflow would potentially enable the cooperative tuning of chemical composition and processing conditions to realize materials personalized for an individual user or a high-value, low-volume application.

A burgeoning form of polymer processing is additive manufacturing (AM), where customized finished polymeric parts can be produced using small footprint and user-friendly infrastructure.[2] Filament printing AM leverages layer-by-layer deposition to build complex shapes, but its reliance on presynthesized thermoplastics with a narrow range of melt viscosities limits the breadth of polymers and subsequent material properties amenable to this approach.[3−5] Vat photopolymerization 3D printing, in contrast, is a versatile type of AM that produces thermosets from customizable resins with a high resolution. Vat photopolymerization demands rapid photocuring of low-viscosity liquid formulations to produce parts at a reasonable rate; consequently, photoinitiated free radical polymerization of acrylates is an ideal synthetic platform due to its fast kinetics and constitutes the majority of the chemistry used in this approach.[6−10] Under the current paradigm, commercial users purchase proprietary formulated resins that contain acrylic monomers, cross-linkers, photoinitiators, and other additives; therefore, the user is restricted to the material properties provided by those commercially available resins.

We envisioned integrating polymer synthesis, formulation, and processing into a continuous material production workflow that leverages the advantages of vat photopolymerization for customized polymer manufacturing. To accomplish this goal, we identified semicontinuous batch chemistry (SCBS) as a synthetic technology that can produce a wide variety of polymer precursors in a rapid, automated, and scalable fashion.[11,12] The integration of SCBS and 3D printing would offer the ability to synthesize and formulate custom resins through software-controlled fluid handling and deliver the products directly to the printer for vat photopolymerization; thus creating an automated manufacturing approach that enables the production of custom polymeric parts directly from their small molecule building blocks and provides opportunities to tune polymer structure to specific processing criteria (Figure 1A).

Received: October 4, 2023
Revised: January 2, 2024
Accepted: January 3, 2024
Published: January 26, 2024

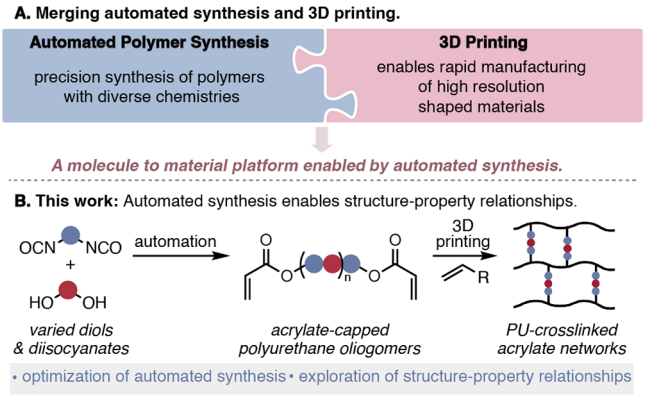

Figure 1. (A) Advantages of integrating automated synthesis and 3D printing as a strategy to unify synthesis and processing. (B) This work: exploration of thermomechanical properties of 3D printed networks cross-linked by a polyurethane cross-linker generated through automated synthesis.

To demonstrate the opportunities provided by integrating polymer synthesis with vat photopolymerization, we identified polyurethanes as a building block for photopolymerization resins. The ability to use different diisocyanate and diol monomers during the synthesis of polyurethanes provides a potentially large structure space of materials to explore, and the known capping of polyurethane oligomers with acrylic groups allows them to be used as cross-linkers in photopolymerization resins.[13−20] Materials made from polyurethane-based resins have good toughness relative to acrylate-only materials, but a systematic exploration of structure−property relationships has not been reported. Key to this work was the orthogonal reactivity of urethane and radical polymerization, which enabled the polyurethane cross-linker to be synthesized in an acrylate solvent that would eventually become the reactive diluent for vat photopolymerization.[21]

Herein, we integrate the synthesis of polyurethane cross-linkers directly to their processing into parts through a combination of SCBS and digital light processing vat photopolymerization 3D printing. These advances are leveraged to evaluate the thermal and mechanical properties of a library of 3D printed acrylic materials cross-linked with custom-synthesized polyurethane oligomers (Figure 1B). This approach enables the printing of resins with short shelf lives due to the intimate connection among synthesis, formulation, and processing. Structure−property studies elucidate trends in how the chemical composition of the polyurethane cross-linker and polymer network architecture impact the resultant mechanical properties. The materials are elastomeric and show low energy loss, which is evaluated through cyclic tensile testing. Overall, this study shows how integrating polymer synthesis with processing enables a systematic evaluation of the material properties and access to new structure spaces.

RESULTS AND DISCUSSION

Oligomer Synthesis Optimization

Lewis acid-catalyzed conditions for the step-growth synthesis of polyurethane (PU) oligomers from diisocyanates and diols were modified to deliver acrylate end-capped oligomers.[22,23] Hydroxy ethyl acrylate (HEA) was included as a monofunctional alcohol to end-cap the oligomers. Optimization of reactant stoichiometries provided conditions that achieved polyurethane oligomers of varying number-average molar masses (M_n), which in turn led to printing formulations with viscosities that spanned the printable range.[24] Reaction optimization was performed using the oligomeric poly(caprolactone) diol (PCL) (M_n − 530 g/mol) and isophorone diisocyanate (IPDI). In order to connect polymer synthesis directly to processing by DLP vat photopolymerization, we leveraged the orthogonal reactivity of urethane and radical chemistry by conducting polymerization using acrylates as the solvent. This solvent then serves as the reactive diluent for 3D printing, which removes any purification or other interventions that would otherwise be required between polymer production and processing. We note that this does limit the identity of the reactive diluent as any functional groups that would react during polyurethane synthesis would impede the step-growth polymerization reaction. We identified a 70% 2-ethylhexyl acrylate (2-EtHex)/30% *N*-vinylpyrrolidone (NVP) as an acrylate mixture that best solubilized the resultant polyurethane oligomers (see Supporting Information for details). To prevent premature cross-linking, the radical inhibitor 4-methoxyphenol was added to all formulations.

Synthesis of a PU oligomer of 3100 g/mol with a dispersity ($Đ$) of 1.89 was accomplished by stirring the alcohol and diisocyanate reactants in the acrylic solvent mixture at a concentration of 1.5 M relative to diisocyanate using 1 mol % of dibutyl tin dilaurate (DBTDL) catalyst (Table 1, entry 1). End-group analysis of the oligomer determined that 31 ± 3% of isocyanate chain ends were left after oligomer synthesis.

Control reactions demonstrated that no oligomers were formed in the absence of a catalyst (Table 1, entry 2) and that the reaction proceeded more slowly at room temperature, which led to lower molar mass (Table 1, entry 3). While it was found that running the reaction in the absence of 4-methoxyphenol was possible, the radical inhibitor was left in the formulation as it had no deleterious impact on M_n or $Đ$ (Table 1, entry 4). Both shorter reaction times and lower catalyst loadings are effective, but to ensure generality across a variety of diols and diisocyanates, the 1 mol % DBTDL loading and 2.5 h reaction time were maintained (Table 1, entries 5 and 6). It was hypothesized that resin viscosity would impact the printing process and the resultant properties of the materials, so reactions at both 1.0 and 2.0 M were assessed; these conditions delivered PU oligomers with similar molar mass while showing the expected trends in viscosity—lower and higher viscosity relative to 1.5 M, respectively (Table 1, entries 7 and 8).

Semicontinuous Batch Synthesis of Polyurethane Oligomers

To integrate polymer synthesis and manufacturing, a semicontinuous batch PU polymerization process was developed that enabled the delivery of freshly synthesized PU resins directly into the bed of the 3D printer. SCBS was chosen for this application due to the long reaction time and large viscosity increase of the resins during polymerization.[11,12,25,26] For the SCBS setup, fluid handling enabled by peristaltic pumps transferred reagents to a stirred reactor;[27−29] after polymerization, the PU oligomer dissolved in acrylates are pumped directly into the resin bed of the 3D printer and processed (a more detailed description of the experimental setup can be found in SI) (Figure 2). The entire sequence was automated; therefore, starting the pumps resulted in the synthesis and processing of PU oligomers without any

https://doi.org/10.1021/acspolymersau.3c00033
ACS Polym. Au 2024, 4, 120−127

Table 1. Optimization of the Synthesis of Acrylate-Capped Polyurethane Oligomers[c]

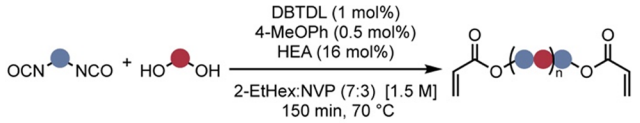

Entry	Deviation from Standard Condition	M_n (g/mol)[a]	M_w (g/mol)[a]	$Đ$[a]	Viscosity (cP)[b]
1	none	3,100	5,800	1.89	710 ± 40
2	no DBTDL	800	1,000	1.34	360 ± 1
3	at room temperature	1,700	2,700	1.63	473 ± 5
4	no 4-methoxyphenol	3,100	5,800	1.87	810 ± 50
5	1 h instead of 2.5 h	2,900	5,400	1.85	870 ± 20
6	0.5 mol% DBTDL	3,000	5,500	1.88	953 ± 45
7	1.0 M reactive diluent	3,000	5,800	1.96	455 ± 2
8	2.0 M reactive diluent	2,800	5,300	1.87	3750 ± 30
9	prepared in flow	3,400	6,700	1.95	1120 ± 30

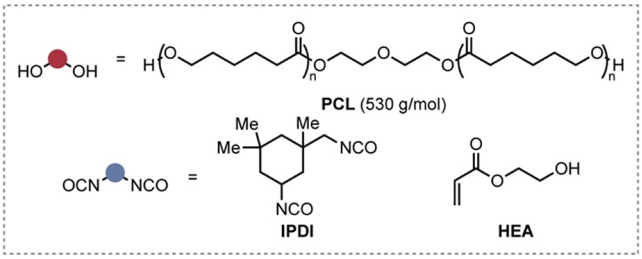

[a]Determined by size exclusion chromatography (SEC) with a refractive index (RI) detector using poly(styrene) standards. [b]Determined by rheology in triplicate. M_n = number-average molar mass, M_w = weight-average molar mass, $Đ$ = dispersity. [c]DBTDL = dibutyl tin dilaurate, 4-MeOPh—4-methoxyphenol, 2-EtHex = 2-ethylhexyl acrylate, NVP = *N*-vinylpyrrolidone.

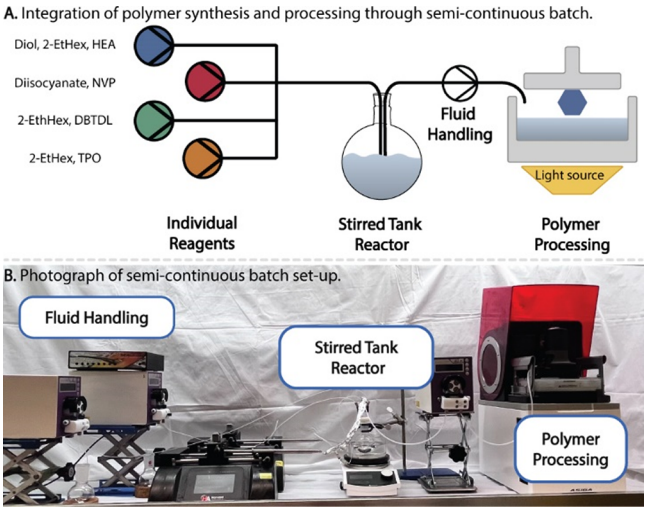

Figure 2. Automated synthesis integrated with a 3D printer. (A) Graphical representation of a semicontinuous batch synthesis setup, where reagents are pumped into a stirred tank reactor, allowed to react for a designated period of time, and then pumped into the printer for polymer processing. (B) Picture of an automated SCBS setup used for resin production.

additional user intervention. PU oligomers prepared in the semicontinuous batch setup delivered similar molar mass and $Đ$ to the material prepared in the traditional batch reaction setup (Table 2, entry 9).

Printing Polyurethane Acrylate Materials

To 3D print the oligomers, diphenyl(2,4,6-trimethylbenzoyl)-phosphine oxide (TPO) was added directly to the completed polyurethane oligomer reactions and stirred for at least 30 min at room temperature in the dark. TPO is a common, commercial photoinitiator for free radical polymerization that absorbs the 405 nm light used by the printer.[30] Different weight % (wt %) loadings of TPO were evaluated by photodifferential scanning calorimetry (photoDSC) to determine the rate and extent of photocuring (Table S1 and Figure S11). It was found that 0.5 wt % of TPO led to the highest degree of photocuring with a 5 s irradiation time at 10 mW/cm^2 without overcuring. The gel point was also studied at different photoinitiator loadings by photorheology; all formulations had rapid modulus crossover points of around 2 s of irradiation (Table S1 and Figures S12—S14).

After formulation, the resins were printed using a digital light processing (DLP) vat photopolymerization printer equipped with 405 nm light. Materials were printed into 1 mm thick sheets with a layer height of 0.05 mm using an exposure time of 5 s and a light intensity of 10 mW/cm^2. After printing, materials were washed with *iso*-propanol to remove unreacted resin and postcured for 5 min with 385 nm light. All materials were subjected to Soxhlet extraction with diethyl ether for 1 h at 70 °C to determine the gel fraction; gel fractions of greater than 93% were found for all materials, indicating a high degree of network formation under printing conditions (Scheme 1).

Synthesis and Characterization of a Library of PU Materials

With robust PU oligomer synthesis conditions for both batch and semicontinuous batch established, a library of materials was designed that incorporated different diols and diisocyanates with the intention of elucidating structure—property relationships. Two aliphatic diisocyanates, IPDI and hexamethylene diisocyanate (HDI), were chosen because they are known to lead to resins with relatively low viscosities compared to aromatic diisocyanates, which was hypothesized to be enabling for DLP vat photopolymerization 3D printing. PCL was chosen as a representative aliphatic polyester monomer, which is a class of materials that are known to lead to high modulus and strength in PU materials.[17] Poly(tetramethylene glycol) (PTMG) was used as a soft polyether monomer that has been shown to improve the elasticity of materials.[14] Finally, bisphenol A ethoxylate (BPAE) was used as a nontoxic variant of BPA, which has been shown to lead to improved materials' performance.[31] Beyond varying the monomers and their relative ratios in the oligomer library, different molar masses were targeted, and materials were made at both 1.5 and 2.0 M oligomer in the reactive diluent to interrogate the impact of concentration on properties.

All resins were formulated on a scale compatible with DLP vat photopolymerization 3D printing (70 mmol scale, ~50 mL of resin) and subjected to SEC analysis. Viscosity was measured by shear rheology to determine the boundary conditions for formulations that could be printed (Table 2). Lower molar mass oligomers (2000 g/mol) were readily achieved (Table 2, entry 1), and higher molar mass oligomers (5100 g/mol) were also possible (Table 2, entry 3). Accessing PUs above 5100 g/mol using simple modifications to the standard reaction conditions was not possible, which could be

https://doi.org/10.1021/acspolymersau.3c00033
ACS Polym. Au 2024, 4, 120—127

Table 2. Scope of Materials Printed and Characterized[e]

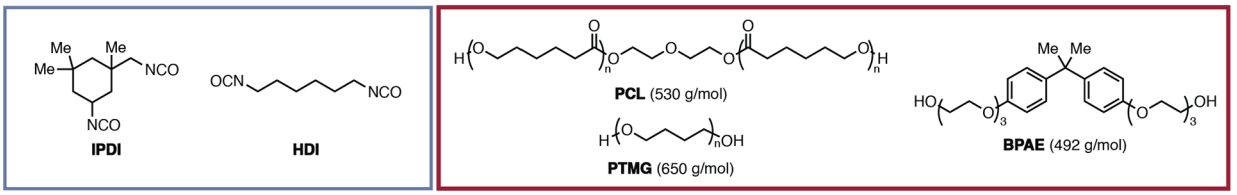

Entry	Diol	Isocyanate	Deviations	M_n (g/mol)[a]	T_g (°C)[b]	$T_{d,5\%}$ (°C)[c]	σ_B (MPa)[d]	ε_B (%)[d]	Toughness (MPa)[d]
Prepared in Batch									
1	PCL	IPDI	target lower M_n	1,800	-2	260	3.9 ± 0.6	180 ± 20	3.2 ± 0.7
2	PCL	IPDI	-	3,600	-7	246	1.7 ± 0.2	180 ± 10	1.6 ± 0.2
3	PCL	IPDI	target higher M_n	5,100	-10	265	1.8 ± 0.3	280 ± 20	2.5 ± 0.5
4	PCL	IPDI	2.0 M	3,000	-7	263	3.3 ± 0.5	350 ± 30	5 ± 1
5	PCL	IPDI:HDI (1:1)	-	3,000	-23	267	1.8 ± 0.3	140 ± 20	1.4 ± 0.3
6	PCL	IPDI:HDI (1:4)	-	3,000	-28	262	1.4 ± 0.3	120 ± 15	0.9 ± 0.3
7	PCL:BPAE (1:1)	IPDI	-	3,300	9	271	12 ± 1	350 ± 20	17 ± 2
8	PCL:PTMG (1:1)	IPDI	-	3,500	-9	276	5 ± 2	240 ± 50	5 ± 3
9	PTMG	IPDI	-	3,300	-24	293	2.5 ± 0.4	170 ± 20	2.2 ± 0.5
10	PTMG	IPDI	target lower M_n	2,200	2	294	7 ± 1	190 ± 20	6 ± 1
11	PTMG	IPDI	2.0 M	3,500	-29	284	3.4 ± 0.5	140 ± 10	2.3 ± 0.4
12	PTMG	IPDI:HDI (1:1)	-	3,400	-50	297	1.4 ± 0.2	120 ± 10	0.8 ± 0.1
13	PTMG:BPAE (1:1)	IPDI	-	3,400	10	288	5.4 ± 0.6	270 ± 20	6.3 ± 0.8
Prepared in Semi-continuous Batch Synthesis									
1f	PCL	IPDI	target lower M_n	1,800	2	278	4.8 ± 0.6	214 ± 9	4.2 ± 0.6
2f	PCL	IPDI	-	3,400	-9	273	2.1 ± 0.2	210 ± 20	2.1 ± 0.4
4f	PCL	IPDI	2.0 M	2,000	-8	267	3.5 ± 0.6	310 ± 30	4.1 ± 0.9
Formulations Enabled by Semi-continuous Batch Synthesis									
14	PCL	HDI	-	3,300	-33	276	1.2 ± 0.1	100 ± 20	0.7 ± 0.2
15	PCL:BPAE (1:4)	IPDI	-	4,200	20	260	6.3 ± 0.8	290 ± 20	9 ± 2
16	BPAE	IPDI	-	2,700	27	261	9 ± 1	210 ± 20	12 ± 2
17	PTMG:BPAE (1:4)	IPDI	-	2,600	20	269	8.0 ± 0.7	270 ± 5	9.9 ± 0.5

[a]Determined by SEC using RI against poly(styrene) standards. [b]Determined by DSC. [c]Determined by TGA. [d]Determined by uniaxial tensile testing 0.05 mm/s strain rate, 500 N load cell, average of five samples; M_n = number-average molecular weight, T_g = glass transition temperature, $T_{d,5\%}$ = temperature at 5% mass loss, σ_B = stress at break, ε_B = strain at break. [e]Standard formulation: 1 mol % DBTDL, 0.5 mol % 4-methoxyphenol, HEA, 1.5 M EtHex:NVP (7:3), 70 °C, 2.5 h, 0.5 wt % TPO. Targeting 4000 g/mol.

Scheme 1. Photoinitiated Free Radical Polymerization To Form Acrylate Networks with Polyurethane Cross-Linkers

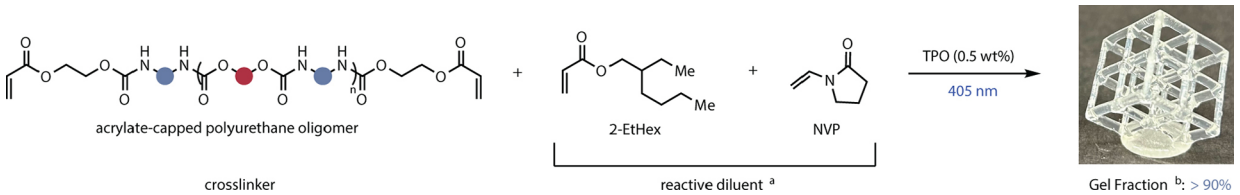

[a]Reactive diluent contains 70 mol % 2-EtHex and 30 mol % NVP. [b]Gel fraction determined by Soxhlet extraction after 3D printing and post-curing.

due to chain termination reactions that occur in the current formulation (see Supporting Information for details). As expected, higher concentration materials led to more viscous resins (Table 2, entries 4 and 11), but they were still printable, although **11** did require heating the printer bed to 35 °C.

We found that several of the target formulations with high percentages of HDI as the diisocyanate solidified upon being left at room temperature for more than 16 h. Additionally, formulations with high percentages of BPAE as the diol component underwent phase separation (for a complete list of materials tried that were unable to be printed, see Supporting Information). For these materials, we leveraged SCBS to synthesize and print the materials in an automated manner. First, to ensure batch and SCBS provided materials with analogous properties, a subset of the materials was made by both methods (entries 1, 2, 4, 1f, 2f, and 4f). These three PU oligomers had nearly identical molar masses in each case, and the subtle differences between their thermal and mechanical properties were statistically insignificant using a Kolmogorov–Smirnov test (Figures S17–S19). This indicates that the materials created with SCBS are analogous to those of their batch counterparts.

Pumping of the resin from the stirred reactor at elevated temperature to the vat would decrease the time between synthesis and printing and provide constant shear mixing, which we hypothesized would mitigate the solidification and

https://doi.org/10.1021/acspolymersau.3c00033
ACS Polym. Au 2024, 4, 120–127

phase separation of resins that is typically experienced during slow cooling or storage that occurs with resins made in batch.[32−34] To evaluate this hypothesis, several materials were targeted in SCBS that were not stable to multihour storage when made through standard batch conditions. Resins that phase separated immediately after or during batch synthesis were not attempted in SCBS. First PCL-HDI, a resin that solidified overnight, was successfully synthesized, formulated into a resin, and printed under automated conditions. SCBS was used to synthesize PCL:BPAE(1:4)-IPDI, PTMG:BPAE (1:4), and BPAE-IPDI (entries 14−17, Table 2), all of which phase separated upon storage for >10 h. Therefore, the semicontinuous batch synthesis and processing of PU oligomers circumvented the short shelf life of a number of formulations, which provided a more thorough investigation of structure−property relationships.

In total, 17 distinct materials were prepared and characterized, 4 of which were accessible only by SCBS and processing (Table 2). Differential scanning calorimetry (DSC) was used to determine the glass transition temperature (T_g) for all of the materials; most of the materials had T_g values below room temperature with the exception of materials with high incorporation of BPAE (Table 2, entries 7, 15, and 16). Additionally, the 5% mass loss temperature ($T_{d,5\%}$) was determined by thermal gravimetric analysis (TGA). While the printed materials exhibited a range of $T_{d,5\%}$s, they were all most consistent with the initial degradation of the acrylate portion of the materials rather than the high decomposition temperatures characteristic for polyurethanes. Given the mixed composition of these materials, two distinct regimes can be observed in the TGA traces consistent with initial thermal degradation of the acrylate portion followed by subsequent degradation of the polyurethane materials (see Figures S71−S90). Both DSC and TGA measurements were also made after Soxhlet extraction, and minimal differences were observed for either the T_g or $T_{d,5\%}$.

Both oscillatory rheology and uniaxial tensile testing measurements were made using discs or dogbones, respectively, which were cut from 1 mm thick printed sheets. A series of temperature, strain, and frequency measurements were performed to determine the storage modulus and molar mass between cross-links of the printed materials (see Tables S7 and S8). From uniaxial tensile testing, stress and strain at break as well as the strain energy density (i.e., toughness) was determined for all the materials. The majority of the tensile curves showed no plastic deformation with the exception of the materials with 80 and 100% BPAE incorporation (Table 2, entries 15 and 16; see the SI for tensile curves). The 17 distinct formulations delivered stress at break (σ_B) values ranging from 1.2 to 12 MPa and strain at break (ε_B) ranging from 100 to 350%, illustrating how the structural variation of the polyurethanes oligomers results in distinct changes in mechanical properties (Figure 3).

Structure−Property Relationships

To understand the influence of the chemical composition of the PU cross-linkers, we synthesized a polymer network using polypropylene glycol (PPG) end-capped with acrylate groups as a cross-linker (Section 6 in SI). Given that PPG would provide a network with similar connectivity and molar mass between cross-links but does not contain groups that will have strong interchain interactions (e.g., carbamates), we hypothesized that the difference in properties between a material made

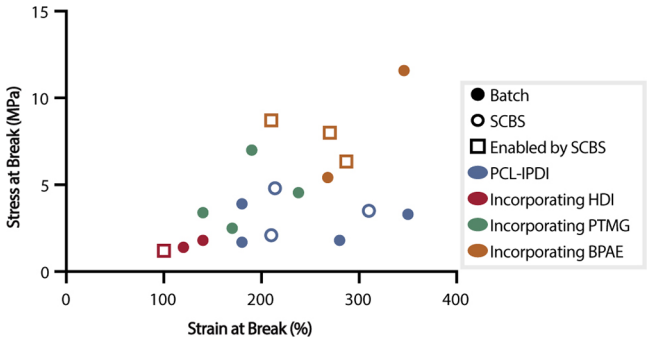

Figure 3. Scope of stress and strain at break values, where each data point represents a material fracture. All stress and strain values are the average of five samples.

with PPG and a PU cross-linker would provide insight into the role chemical composition plays on material properties. We were not able to match the dispersity of the PPG cross-linker with the PU materials given they are made through different mechanisms, so the mesh sizes of the networks was different. The network printed using the PPG cross-linker had lower values for stress and strain at break (σ_B = 0.47 MPa, ε_B = 52%, Figure S30) compared to entry 3, which is its closest analogue for molar mass between cross-links. We hypothesize that a contributing factor to the differences in properties was the lack of interchain interactions in the PPG cross-linked material, providing evidence that the interchain interactions present in 3D printed PU networks are an important factor in achieving materials with attractive thermomechanical properties.

Altering both the molar mass and the concentration of the PU cross-linker had an impact on the tensile properties (Figure 4A). For the materials comprised of PCL as the diol component and IPDI as the diisocyanate component, lower molar mass cross-linkers led to higher stress at break, while higher molar mass led to increased strain at break. Given both cross-linkers are well below their entanglement molecular weight, these trends fit the theory of rubber elasticity where the finite extensibility of networks stands is related to the molar mass between cross-links.[35] Increasing the concentration of oligomers in the reactive diluent led to an increase in stress for both samples tested, as would be expected given the increase in cross-link density. Interestingly, the materials with a higher concentration of PU cross-linkers demonstrated either a higher (entry 4) or similar (entry 11) strain at break. In these cases, we attribute this behavior to the change in chemical composition as PU cross-linker concentration increases, where the interchain interactions (e.g., hydrogen bonding and/or dipole−dipole interactions) presumably play a role in toughening the material.[36]

Leveraging the library of data reported herein, we sought to understand the role of the diol in the PU cross-linkers. Overall, similar trends in mechanical properties were observed when either PCL or PTMG was used as the diol, although PTMG-IPDI oligomers targeting 8000 g/mol were unable to be printed due to the high viscosity of this material even at elevated printing temperatures (Figure S20). In contrast, incorporating BPAE as the diol component into the PU cross-linkers led to the strongest materials in the library (Figure 4C). Moving to 50 mol % BPAE with 50 mol % PCL gave a material with both significantly improved strain and stress at break. The increase in T_g indicates a decrease in chain flexibility, and the aromatic ring in BPAE is hypothesized to further increase

https://doi.org/10.1021/acspolymersau.3c00033
ACS Polym. Au 2024, 4, 120−127

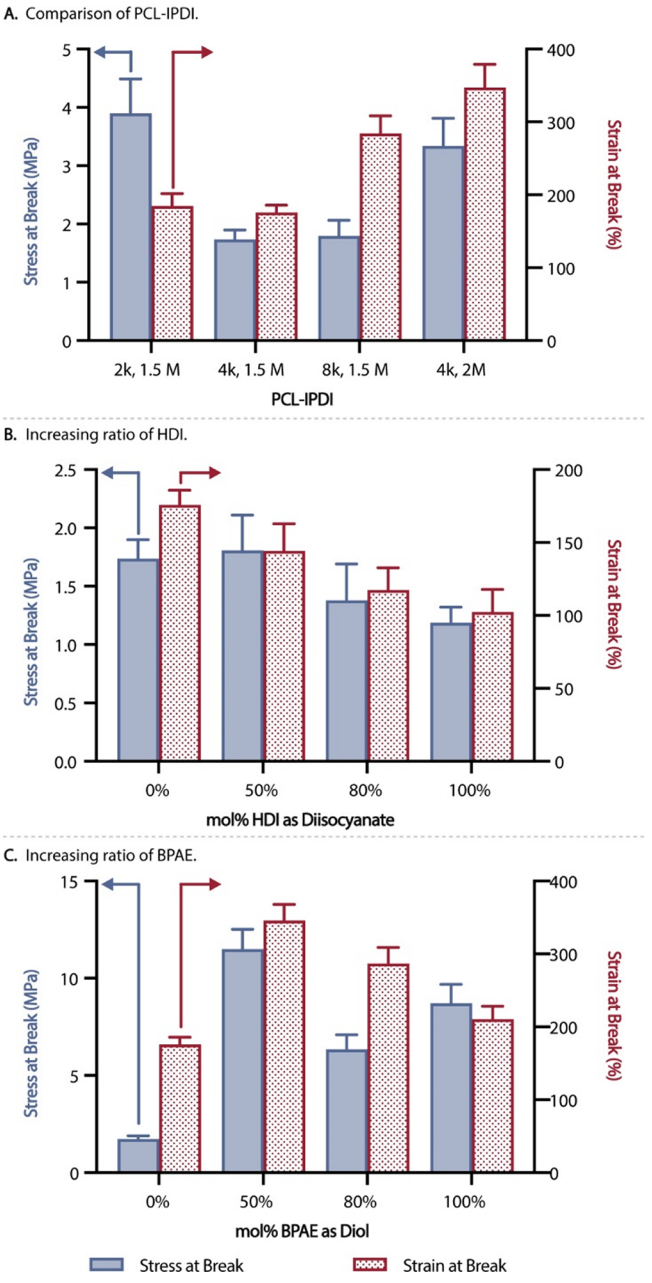

Figure 4. Structure–property relationships from uniaxial tensile testing for (A) PCL-IPDI materials of different molecular weights and concentrations. (B) PCL-IPDI:HDI materials with different incorporations of HDI. (C) PCL:BPAE-IPDI materials with different incorporations of BPAE. Data are the average of five measurements, and error bars indicate standard deviation.

interchain interactions; we propose that the combination of these factors leads to enhanced properties. Exploring this trend further was not possible using traditional batch chemistry, as resin formulations phase separated immediately after synthesis. Here, the SCBS reactor provided access to these otherwise challenging materials in order to further understand structure–property relationships. While the stress and strain at break for materials with 80 and 100% BPAE synthesized in the semicontinuous batch reactor were slightly lower than the 50% BPAE material, the properties remained higher than those of materials incorporating just PCL or PTMG. Similar trends were observed for PTMG materials with increasing BPAE content (Figure S22).

When systematically exploring the influence of the diisocyanate component by increasing the ratio of HDI to IPDI, it was found that both strain and stress at break decreased with an increase in HDI content (Figure 4B). We also observed that formulations that contained HDI were less soluble, indicating that aggregation of the oligomers facilitated by the less sterically encumbered diisocyanate may embrittle the materials and result in poor properties. Using HDI as the sole diisocyanate was only possible with the semicontinuous batch reaction conditions due to rapid solidification; ultimately, this material had the worst properties of any of the materials tested in this study. Similar trends were observed when increasing the HDI ratio with PTMG as a diol, but 80 and 100% HDI formulations solidified in both the batch and SCBS reactors, precluding their further study (Figure S21).

Hysteresis Measurements

Typical 3D printed acrylate materials tend to be brittle, but the PU acrylate resins studied herein showed elastomeric tensile behavior with no observable plastic deformation (see Supporting Information for tensile curves for PU material, Figures S119–S136). To test the elasticity of these materials, a representative material—PCL-IPDI at 2 M (entry 4), which had the highest observed strain at break—was subjected to cyclic loading and unloading studies. In 50% strain increments at a Hencky strain rate of 0.003 s^{-1}, dogbones cut from 1 mm thick printed sheets underwent tension and compression cycles up to 250% strain (Figure 5). This material showed a good

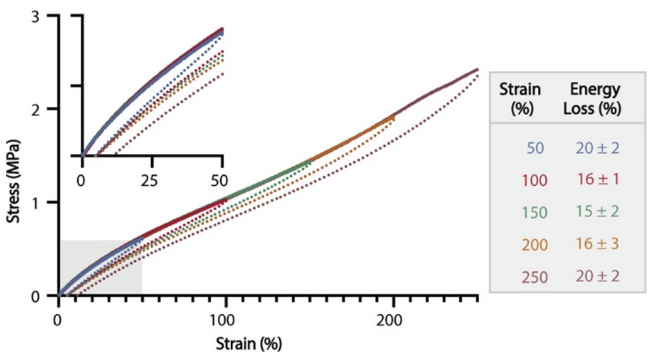

Figure 5. Hysteresis data were from PCL-IPDI-2M. Hysteresis curves are representative of one run. Energy loss measurements are the average of three measurements on different samples.

overlap in repeated tension cycles. The energy loss for each cycle was quantified by comparing the area under the curve for tension to that under the curve for compression. This material showed only a modest energy loss of between 15 and 20%. While these cyclic tensile tests were performed on only one material, it is hypothesized that most of the materials studied here would exhibit similar behavior, given their consistent lack of plastic deformation. The exception would be the materials with high BPAE (80 and 100 mol %) incorporation, which do show initial plastic deformation in the tensile curves (Figures S134–S136).

CONCLUSIONS

Connecting polymer synthesis and processing through a semicontinuous batch process enabled the synthesis of a library of acrylate-capped polyurethane oligomers that served

https://doi.org/10.1021/acspolymersau.3c00033
ACS Polym. Au 2024, 4, 120–127

as cross-linkers in 3D printed materials. The resultant materials delivered a range of thermal and mechanical properties. Structure−property studies provided insight into how incorporating an increasing amount of rigid aromatic diols leads to stronger materials, and incorporating symmetric diisocyanates leads to solidification of the materials and less attractive mechanical properties. Additionally, it was observed that altering the length of the polyurethane cross-linkers plays a significant role in the overall final properties of the materials, as shorter cross-linkers led to stiffer and less extensible materials, and longer cross-linkers resulted in weaker and more elastic materials. The materials were found to be elastic with a relatively low energy loss between tension and compression cycles. All together these detailed structure−property studies were enabled by coupling synthesis and processing, as the semicontinuous reactor provided routine access to materials that would otherwise have short shelf lives.

EXPERIMENTAL SECTION

Detailed synthetic procedures for polyurethane oligomers along with procedures for DLP additive manufacturing and characterization data for polymerizations and polyurethane elastomers can be found in the Supporting Information. Specifics for NMR spectroscopy, GPC, infrared spectroscopy, DSC, TGA, rheology, and tensiometry are also present in the Supporting Information.

Representative Procedure for Polyurethane Oligomer Synthesis in Batch

The procedure for the synthesis of the resin found in Table 1, entry 1 follows, with other resins using different chemical identities and ratios of diols and diisocyanates, as detailed in the Supporting Information.

In an oven-dried 100 mL round bottom flask equipped with a dry PTFE coated stir bar, PCL diol (12.9 g, 24.4 mmol, 0.34 equiv), HEA (1.29 mL, 11.28 mmol, 0.16 equiv), 4-methoxy phenol (44.32 mg, 0.35 mmol, 0.05 equiv), 2-ethylhexyl acrylate (18.57 mL), and *N*-vinyl pyrrolidone (6.77 mL) were added and heated to 70 °C until homogeneous. IPDI (7.47 mL, 35.64 mol, 0.5 equiv) was added and stirred for 5 min. Subsequently, DBTDL (149 μL, 1 mol %) was added and the reaction vessel sealed with a septa equipped with a vent needle. After stirring for 2.5 h, the reaction mixture was cooled to room temperature and an aliquot of the reaction was taken for GPC and viscosity measurements. It is important to note that due to this connection between processing and synthesis previously mentioned, amounts of potentially toxic tin compounds may still remain in the printed parts, and common PPE is suggested when handling printed parts.

Representative Procedure for Semicontinuous Batch Synthesis

The procedure for the semicontinuous batch synthesis of the resin found in Table 1, entry 1 follows, with other resins using different chemical identities and ratios of diols and diisocyanates, as detailed in the Supporting Information.

Two stock solutions—(1) diol, hydroxyethyl acrylate, 4-methoxyphenol, and 2-ethylhexyl acrylate and (2) diisocyanate and *N*-vinylpyrrolidone—were pumped into a round-bottom flask at a flow rate of 1 mL/min using peristaltic pumps. The solution was stirred for 1 min, and then, stock solution 3 of 2-ethylhexyl acrylate and dibutyltin dilaurate was added at 1 mL/min using a syringe pump. The reaction solution was then allowed to stir for 150 min at 70 °C. Subsequently, stock solution 4 consisting of diphenyl(2,4,6-trimethylbenzoyl)phosphine oxide and 2-ethylhexyl acrylate was added to the reaction solution using a syringe pump and stirred for 1 h to ensure adequate mixing. Then, the entire solution was pumped from the round bottom into the vat of the DLP printer using a peristaltic pump at a flow rate of 2 mL/min.

Stock solution 1: PCL (19.84 g, 37.43 mmol), 2-EtHex (40.08 mL), HEA (5.19 mL, 45.14 mmol), 4MeO-Ph (102.69 mg).
Stock solution 2: IPDI (17.35 mL, 82.57 mmol), NVP (17.54 mL).
Stock solution 3: 2-EtHex (4 mL), DTBDL (343 μL, 1.65 mmol).
Stock solution 4: 2-EtHex (4 mL), TPO (523 mg).

ASSOCIATED CONTENT

Supporting Information

The Supporting Information is available free of charge at https://pubs.acs.org/doi/10.1021/acspolymersau.3c00033.

Experimental procedures, characterization data, photorheology data, ^{1}H NMR and ^{13}C NMR spectra, GPC trace, DSC data, TGA data, rheology data, strain and frequency sweeps, overlay of the five tensile measurements, viscosity values for resins, mechanical data from the average of five samples, and decomposition temperatures determined by TGA (PDF)

AUTHOR INFORMATION

Corresponding Author

Frank A. Leibfarth − *Department of Chemistry, The University of North Carolina at Chapel Hill, Chapel Hill, North Carolina 27514, United States;* orcid.org/0000-0001-7737-0331; Email: FrankL@email.unc.edu

Authors

Johann L. Rapp − *Department of Chemistry, The University of North Carolina at Chapel Hill, Chapel Hill, North Carolina 27514, United States*

Meredith A. Borden − *Department of Chemistry, The University of North Carolina at Chapel Hill, Chapel Hill, North Carolina 27514, United States*

Vittal Bhat − *Department of Chemistry, The University of North Carolina at Chapel Hill, Chapel Hill, North Carolina 27514, United States*

Alexis Sarabia − *Department of Chemistry, The University of North Carolina at Chapel Hill, Chapel Hill, North Carolina 27514, United States*

Complete contact information is available at: https://pubs.acs.org/10.1021/acspolymersau.3c00033

Author Contributions

J.L.R. and M.A.B. contributed equally. J.L.R.: conceptualization (equal), formal analysis (equal), writing−original draft (supporting), writing−review and editing (equal); M.A.B.: conceptualization (equal), formal analysis (equal), writing−original draft (lead), writing−review and editing (equal); V.B.: formal analysis (supporting), writing−review and editing (supporting); A.S.: conceptualization (equal), formal analysis (supporting); F.A.L.: conceptualization (equal), funding acquisition (lead), project administration (lead), supervision (lead), writing−review and editing (equal).

Notes

The authors declare no competing financial interest.

ACKNOWLEDGMENTS

This work was supported by the United States Department of Energy/National Nuclear Security Administration Kansas City National Security Campus, operated by Honeywell Federal Manufacturing & Technologies, LLC, under Contract Number DE-NA0002839, and the National Science Foundation under a

CAREER award (CHE-1847362). We are grateful to Prof. Theo Dingemans, Prof. Sergei Sheiko, and Prof. Wei You for granting us access to the materials' characterization instrumentation. We would like to thank Dr. Will Daniels and Dr. Mitch Maw for helpful discussions about tensile testing of elastomers and cyclic tensile testing, respectively.

REFERENCES

(1) Xanthos, M. Sect 2 Polym Sci Technology. In *Applied Polymer Science: 21st Century*; Craver, C., Carraher, C., Eds.; 2000; pp 355−371.
(2) Pereira, T.; Kennedy, J. V.; Potgieter, J. A Comparison of Traditional Manufacturing vs Additive Manufacturing, the Best Method for the Job. *Procedia Manuf.* **2019**, *30*, 11−18.
(3) Tully, J. J.; Meloni, G. N. A Scientist's Guide to Buying a 3D Printer: How to Choose the Right Printer for Your Laboratory. *Anal. Chem.* **2020**, *92* (22), 14853−14860.
(4) Lipkowitz, G.; Samuelsen, T.; Hsiao, K.; Lee, B.; Dulay, M. T.; Coates, I.; Lin, H.; Pan, W.; Toth, G.; Tate, L.; Shaqfeh, E. S. G.; DeSimone, J. M. Injection Continuous Liquid Interface Production of 3D Objects. *Sci. Adv.* **2022**, *8* (39), 1−12.
(5) Tumbleston, J. R.; Shirvanyants, D.; Ermoshkin, N.; Janusziewicz, R.; Johnson, A. R.; Kelly, D.; Chen, K.; Pinschmidt, R.; Rolland, J. P.; Ermoshkin, A.; Samulski, E. T.; Desimone, J. M. Continuous Liquid Interface Production of 3D Objects. *Science* **2015**, *347* (6228), 1349−1352.
(6) Zhang, J.; Xiao, P. 3D Printing of Photopolymers. *Polym. Chem.* **2018**, *9* (13), 1530−1540.
(7) Bagheri, A.; Jin, J. Photopolymerization in 3D Printing. *ACS Appl. Polym. Mater.* **2019**, *1* (4), 593−611.
(8) Boydston, A. J.; Cui, J.; Lee, C. U.; Lynde, B. E.; Schilling, C. A. 100th Anniversary of Macromolecular Science Viewpoint: Integrating Chemistry and Engineering to Enable Additive Manufacturing with High-Performance Polymers. *ACS Macro Lett.* **2020**, *9* (8), 1119−1129.
(9) Appuhamillage, G. A.; Chartrain, N.; Meenakshisundaram, V.; Feller, K. D.; Williams, C. B.; Long, T. E. 110th Anniversary: Vat Photopolymerization-Based Additive Manufacturing: Current Trends and Future Directions in Materials Design. *Ind. Eng. Chem. Res.* **2019**, *58* (33), 15109−15118.
(10) Ligon, S. C.; Liska, R.; Stampfl, J.; Gurr, M.; Mülhaupt, R. Polymers for 3D Printing and Customized Additive Manufacturing. *Chem. Rev.* **2017**, *117* (15), 10212−10290.
(11) Tonhauser, C.; Natalello, A.; Löwe, H.; Frey, H. Microflow Technology in Polymer Synthesis. *Macromolecules* **2012**, *45* (24), 9551−9570.
(12) Plutschack, M. B.; Pieber, B.; Gilmore, K.; Seeberger, P. H. The Hitchhiker's Guide to Flow Chemistry. *Chem. Rev.* **2017**, *117* (18), 11796−11893.
(13) Deng, Y.; Li, J.; He, Z.; Hong, J.; Bao, J. Urethane Acrylate-Based Photosensitive Resin for Three-Dimensional Printing of Stereolithographic Elastomer. *J. Appl. Polym. Sci.* **2020**, *137* (42), 1−12.
(14) Peng, S.; Li, Y.; Wu, L.; Zhong, J.; Weng, Z.; Zheng, L.; Yang, Z.; Miao, J. T. 3D Printing Mechanically Robust and Transparent Polyurethane Elastomers for Stretchable Electronic Sensors. *ACS Appl. Mater. Interfaces* **2020**, *12* (5), 6479−6488.
(15) De Souza, F. M.; Kahol, P. K.; Gupta, R. K. Introduction to Polyurethane Chemistry. *ACS Symp. Ser.* **2021**, *1380*, 1−24.
(16) Engels, H. W.; Pirkl, H. G.; Albers, R.; Albach, R. W.; Krause, J.; Hoffmann, A.; Casselmann, H.; Dormish, J. Polyurethanes: Versatile Materials and Sustainable Problem Solvers for Today's Challenges. *Angew. Chem., Int. Ed.* **2013**, *52* (36), 9422−9441.
(17) Akindoyo, J. O.; Beg, M. D. H.; Ghazali, S.; Islam, M. R.; Jeyaratnam, N.; Yuvaraj, A. R. Polyurethane Types Synthesis and Applications-a Review. *RSC Adv.* **2016**, *6* (115), 114453−114482.
(18) Huang, Y.; Zhao, H.; Wang, X.; Liu, X.; Gao, Z.; Bai, H.; Lv, F.; Gu, Q.; Wang, S. Polyurethane-Gelatin Methacryloyl Hybrid Ink for 3D Printing of Biocompatible and Tough Vascular Networks. *Chem. Commun.* **2022**, *58* (49), 6894−6897.
(19) Li, X.; Yu, R.; He, Y.; Zhang, Y.; Yang, X.; Zhao, X.; Huang, W. Self-Healing Polyurethane Elastomers Based on a Disulfide Bond by Digital Light Processing 3D Printing. *ACS Macro Lett.* **2019**, *8* (11), 1511−1516.
(20) Lopez De Pariza, X.; Erdmann, T.; Arrechea, P. L.; Perez, L.; Dausse, C.; Park, N. H.; Hedrick, J. L.; Sardon, H. Synthesis of Tailored Segmented Polyurethanes Utilizing Continuous-Flow Reactors and Real-Time Process Monitoring. *Chem. Mater.* **2021**, *33* (20), 7986−7993.
(21) Allen, M. J.; Lien, H. M.; Prine, N.; Burns, C.; Rylski, A. K.; Gu, X.; Cox, L. M.; Mangolini, F.; Freeman, B. D.; Page, Z. A. Multimorphic Materials: Spatially Tailoring Mechanical Properties via Selective Initiation of Interpenetrating Polymer Networks. *Adv. Mater.* **2023**, *35* (9), 21−23.
(22) Devendra, R.; Edmonds, N. R.; Söhnel, T. Computational and Experimental Investigations of the Urethane Formation Mechanism in the Presence of Organotin(IV) Carboxylate Catalysts. *J. Mol. Catal. A Chem.* **2013**, *366*, 126−139.
(23) Luo, Y.; Gu, M.; Edwards, C. E. R.; Valentine, M. T.; Helgeson, M. E. High-Throughput Microscopy to Determine Morphology, Microrheology, and Phase Boundaries Applied to Phase Separating Coacervates. *Soft Matter* **2022**, *18* (15), 3063−3075.
(24) Rogers, M. E.; Long, T. E.; Turner, S. R. Introduction to Synthetic Methods in Step-Growth Polymers. *Synth. Methods Step-Growth Polym.* **2003**, 1−16.
(25) Junkers, T. Precision Polymer Design in Microstructured Flow Reactors: Improved Control and First Upscale at Once. *Macromol. Chem. Phys.* **2017**, *218* (2), 1−9.
(26) Junkers, T. Precise Macromolecular Engineering via Continuous-Flow Synthesis Techniques. *J. Flow Chem.* **2017**, *7* (3−4), 106−110.
(27) Myers, R. M.; Fitzpatrick, D. E.; Turner, R. M.; Ley, S. V. Flow Chemistry Meets Advanced Functional Materials. *Chem. - A Eur. J.* **2014**, *20* (39), 12348−12366.
(28) Pittaway, P. M.; Ghasemi, G.; Knox, S. T.; Cayre, O. J.; Kapur, N.; Warren, N. J. Continuous Synthesis of Block Copolymer Nanoparticles via Telescoped RAFT Solution and Dispersion Polymerisation in a Miniature CSTR Cascade. *React. Chem. Eng.* **2023**, *8* (3), 707−717.
(29) Le, C. M. Q.; Chemtob, A. Thiol-Ene Emulsion Step Polymerization in a Photochemical Stirred Tank Reactor: Molecular Weight, Cyclization, and Fragmentation. *J. Polym. Sci.* **2023**, *61* (4), 323−333.
(30) Zhang, Y.; Xu, Y.; Simon-Masseron, A.; Lalevée, J. Radical Photoinitiation with LEDs and Applications in the 3D Printing of Composites. *Chem. Soc. Rev.* **2021**, *50* (6), 3824−3841.
(31) Laza, J. M.; Veloso, A.; Vilas, J. L. Tailoring New Bisphenol a Ethoxylated Shape Memory Polyurethanes. *J. Appl. Polym. Sci.* **2021**, *138* (2), 1−10.
(32) Reis, M. H.; Leibfarth, F. A.; Pitet, L. M. Polymerizations in Continuous Flow: Recent Advances in the Synthesis of Diverse Polymeric Materials. *ACS Macro Lett.* **2020**, *9* (1), 123−133.
(33) Reis, M. H.; Varner, T. P.; Leibfarth, F. A. The Influence of Residence Time Distribution on Continuous-Flow Polymerization. *Macromolecules* **2019**, *52* (9), 3551−3557.
(34) Nagaki, A.; Tomida, Y.; Yoshida, J. I. Microflow-System-Controlled Anionic Polymerization of Styrenes. *Macromolecules* **2008**, *41* (17), 6322−6330.
(35) Treloar, L. R. G. *The Physics of Rubber Elasticity*, third ed.; Oxford University Press: 2005.
(36) Polyurethane, N.; Delebecq, E.; Pascault, J.; Boutevin, B.; De Lyon, U. On the Versatility of Urethane/Urea Bonds: Reversibility, Blocked Isocyanate, and Non-isocyanate polyurethane. *Chem. Rev.* **2013**, *113*, 80−118.

https://doi.org/10.1021/acspolymersau.3c00033
ACS Polym. Au 2024, 4, 120−127